

Characterization of Local Critical Current Distribution in Multifilamentary Coated Conductor Based on Reel-to-Reel Scanning Hall-Probe Microscopy

Higashikawa, Kohei
Department of Electrical Engineering, Kyushu University

Uetsuhara, Dai
Department of Electrical Engineering, Kyushu University

Inoue, Masayoshi
Department of Electrical Engineering, Kyushu University

Fujita, Shinji
Fujikura Ltd.

他

<https://hdl.handle.net/2324/7432836>

出版情報 : IEEE Transactions on Applied Superconductivity. 27 (4), pp.6603004-, 2016-12-16.
Institute of Electrical and Electronics Engineers (IEEE)

バージョン :

権利関係 : © 2016 IEEE. Personal use of this material is permitted. Permission from IEEE must be obtained for all other uses, in any current or future media, including reprinting/republishing this material for advertising or promotional purposes, creating new collective works, for resale or redistribution to servers or lists, or reuse of any copyrighted component of this work in other works.





Characterization of Local Critical Current Distribution in Multi-filamentary Coated Conductor Based on Reel-to-reel Scanning Hall-probe Microscopy

Kohei Higashikawa, Dai Uetsuhara, Masayoshi Inoue, Shinji Fujita, Yasuhiro Iijima, and Takanobu Kiss

Abstract— We have carried out the characterization of local critical current distribution in a 113-m-long multi-filamentary coated conductor (CC) based on reel-to-reel scanning Hall-probe microscopy (RTR-SHPM). Patterning multi-filamentary structure on CCs is a key technology for the reduction of AC losses due to magnetization. Recently, this advantage has also been expected for the reduction of the magnetization in a coil winding which has been recognized as a critical problem for HTS magnet applications such as accelerators, MRI, and NMR from the viewpoint of field homogeneity and temporal stability. However, it has been difficult for the conventional techniques such as four-probe method, TAPESTAR™, etc. to make diagnostics for multi-filamentary CCs due to the limitation of spatial resolution. On the other hand, our measurement has an advantage in taking two-dimensional field image. This enabled us to confirm that multi-filamentary structure as well as the corresponding magnetization reduction were successfully achieved in a long-length CC. At the same time, by the estimation of local critical current distribution for each filament, it was also found that there were still some local defects, which affected the global performance of the multi-filamentary CC, even if the probability density of such defects was only in the order of 10^{-5} . These findings will become crucial information for the optimization of fabrication processes of multi-filamentary CCs and for their nondestructive quality assurance.

Index Terms— critical current distribution, multi-filamentary tape, RE-123 coated conductor, RTR-SHPM.

I. INTRODUCTION

RE-123 (RE: Y, Gd, etc.) coated conductors (CCs) have been especially expected for high-field magnet applications such as MRI and NMR by taking advantages of high critical current density against magnetic field and high mechanical strength against the corresponding electromagnetic force. On the other hand, the magnetization and its time variation of CCs have been recognized as a critical problem in such applications from the viewpoint of field homogeneity and temporal stability [1]-[3].

Manuscript received September 6, 2016. This work was partly supported by “JSPS: KAKENHI (16H02334, 16K14216).”

K. Higashikawa, D. Uetsuhara, M. Inoue, and T. Kiss are with the Department of Electrical Engineering, Graduate School of Information Science and Electrical Engineering, Kyushu University, 744 Motoooka, Nishiku, Fukuoka 819-0395, Japan (e-mail: kohei@super.ees.kyushu-u.ac.jp).

S. Fujita and Y. Iijima are with the Fujikura Ltd., Chiba 285-8550, Japan.

Patterning multi-filamentary structure on CCs would become a promising solution for the magnetization issue. In fact, such multi-filamentary CCs have been successfully fabricated by several groups [4]-[6]. Although these are originally for the reduction of AC losses, recently this advantage has also been expected for the compensation of the abovementioned problem in high-field applications [7].

On the other hand, multi-filamentary CCs will have the possibility of damage resulting from their patterning processes such as striation and from the severe influence from local defects because smaller defects block current flow in narrower filaments. Therefore, diagnostics by the characterization of local critical current distribution is especially important for multi-filamentary CCs. However, the conventional technique, i.e., TAPESTAR™ [8], which is well known as a de facto standard method, cannot be directly used for the characterization of multi-filamentary CCs because of the lack of the spatial resolution along the conductor width. Magneto-optic imaging (MOI) [4] also has some difficulty in calibration required for a quantitative analysis for long CCs. Scanning Hall-probe microscopy (SHPM) has shown powerful potential for the diagnostics of multi-filamentary CCs; however the sample length has been limited to several centimeters at this moment [9], [10].

In this study, we applied reel-to-reel scanning Hall-probe microscopy (RTR-SHPM) [11] to the diagnostics of a 113 m long, 4 mm wide CC with 4 filaments. As a result, it was confirmed that the multi-filamentary structure as well as the corresponding magnetization reduction were successfully achieved in such a long-length CC. At the same time, it was also found that there were still some local defects, which affected the global performance of the multi-filamentary CC, although they could not be detected by a TAPESTAR™ machine.

II. MATERIALS AND METHODS

A. Sample: 113-m-long Multi-filamentary CC

Fujikura Ltd. has developed a multi-filamentary CC by scratching its buffer layer along the longitudinal direction [7]. Fig. 1 shows the schematic of the cross-sectional structure of the CC. The GdBCO layer is divided by non-superconductive streaks on the scratches of the buffer layer. Although the

filaments are electrically coupled also by the Cu foil, it is supposed that the magnetization in a DC state would be reduced because current cannot flow across the interface between the filaments at zero-resistance. This will address the above-mentioned problem of magnetization in high-field applications. A 113-m-long, 4-mm-wide, and 4-filamentary CC was selected as the sample.

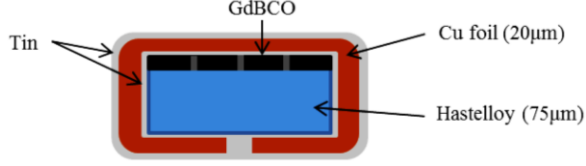


Fig. 1. Schematic diagram of the cross-sectional structure of the multi-filamentary CC fabricated by buffer scratching along longitudinal direction [7].

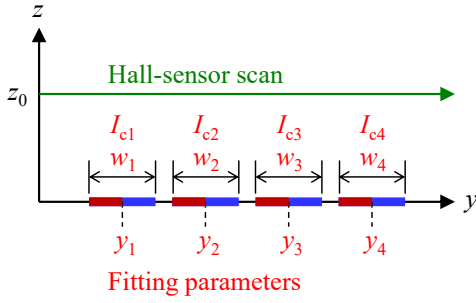


Fig. 2. Illustration of the parameters at the analysis of local critical current estimation.

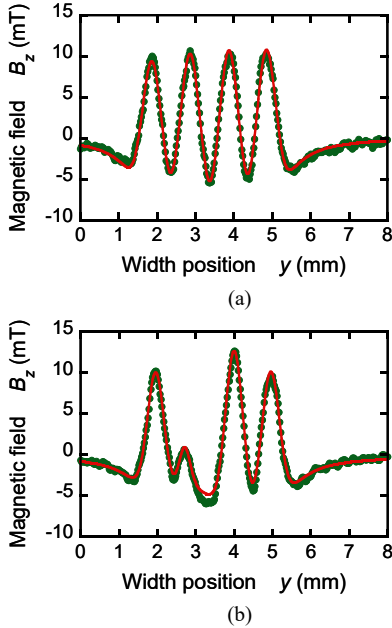


Fig. 3. Fitting results of remanent magnetic field distribution at longitudinal position with (a) balanced filamentary critical currents and (b) unbalanced filamentary critical currents. Measurement data are plotted as symbols, and the solid curves are from equation (1).

B. Measurement of Remanent Magnetic Field Distribution

RTR-SHPM [11] was used for the characterization of the sample. Two-dimensional in-plane distribution of remanent magnetic field of the sample was taken by scanning a Hall sensor in width direction above the fully-magnetized sample traveling in longitudinal direction. Only the component perpendicular to the sample's surface, B_z , was measured. The traveling speed was set to be 24 m/h.

C. Analysis of Local Critical Current Distribution

As a result of the measurement, B_z could be obtained as a function of width position, y , at each longitudinal position, x . Using the parameters shown in Fig. 2 where only the longitudinal components of the magnetization currents are assumed, $B_z(y)$ can be analytically expressed by the Biot-Savart law for the fully-magnetized sample with assuming the critical state model:

$$\begin{aligned}
 B_z(y) &= 4\pi \times 10^{-7} \times \sum_{k=1}^4 \left(\int_{y_k - w_k/2}^{y_k} \frac{I_{ck} / w_k}{2\pi \sqrt{(y-y')^2 + z_0^2}} \frac{(y-y')}{\sqrt{(y-y')^2 + z_0^2}} dy' \right. \\
 &\quad \left. - \int_{y_k}^{y_k + w_k/2} \frac{I_{ck} / w_k}{2\pi \sqrt{(y-y')^2 + z_0^2}} \frac{(y-y')}{\sqrt{(y-y')^2 + z_0^2}} dy' \right) \\
 &= 10^{-7} \times \sum_{k=1}^4 \frac{I_{ck}}{w_k} \ln \left(\frac{\left((y - y_k - w_k/2)^2 + z_0^2 \right) \left((y - y_k + w_k/2)^2 + z_0^2 \right)}{\left((y - y_k)^2 + z_0^2 \right)^2} \right)
 \end{aligned} \tag{1}$$

where I_{ck} , w_k , and y_k are local critical current, width, and width position of each filament at a longitudinal position, respectively. They were dealt as fitting parameters for $B_z(y)$ while the distance between the Hall-sensor scan and the filaments, z_0 , was dealt as a known value. The fitting was done by the Levenberg-Marquardt method, which had been given as a ready-made block in LabVIEW™, with an appropriate set of their initial values. Fig. 3 shows the typical fitting results; the equation describes the measured magnetic field distributions very well. According to this procedure, local critical current at a longitudinal position was estimated for each filament.

III. RESULTS AND DISCUSSION

Fig. 4 shows the longitudinal distributions of critical currents, I_c , in the sample characterized by the conventional techniques: TAPESTAR™ and 4-probe method. TAPESTAR™ shows uniform I_c distribution for this sample. Furthermore, 4-probe method also shows $I_c = \sim 200$ A for every 4.7-m-long section throughout the whole length of the sample. It could be confirmed that such a sophisticated multi-filamentary CC was successfully fabricated by Fujikura Ltd. On the other hand, some I_c drops were detected by the 4-probe method (e.g., around $x = 22, 80, 90$ m, etc.) while no obvious defects were detected by TAPESTAR™. Furthermore, only from these results obtained by the conventional characterization techniques, it is difficult to confirm the quality of a multi-filamentary CC.

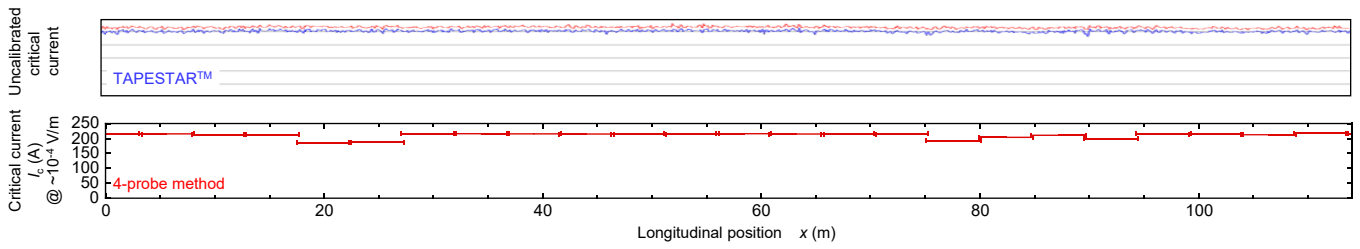


Fig. 4. Longitudinal distributions of critical currents in the sample characterized by the conventional techniques: TAPESTAR™ and 4-probe method.

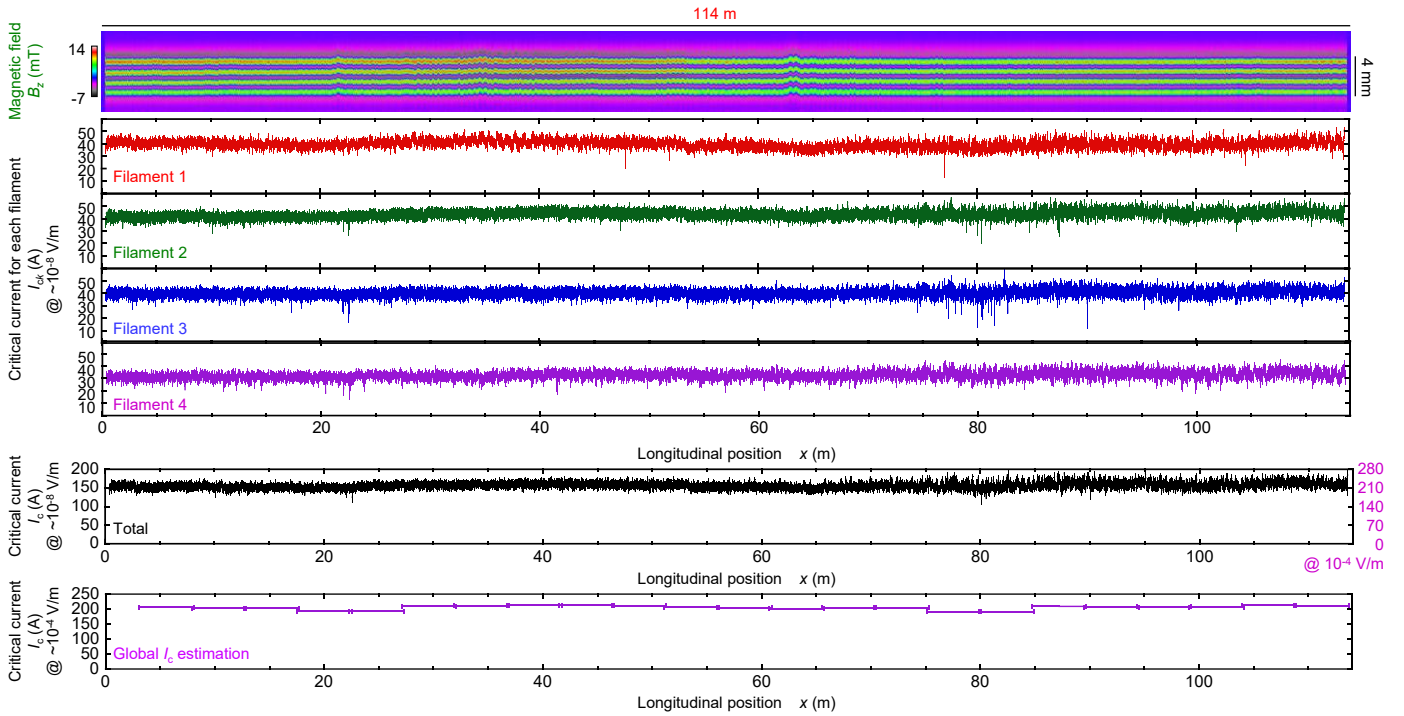


Fig. 5. Characterization results obtained by the RTR-SHPM with the related analyses: remanent magnetic field distribution, local I_c distribution for each filament, that for total I_c , and the corresponding global I_c estimated for every 4.7-m-section in a 113-m-long, 4-mm-wide, and 4-filamentary CC.

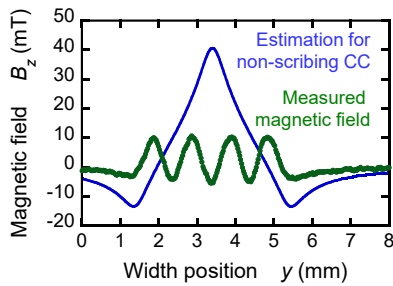


Fig. 6. Comparison magnetization between the multi-filamentary CC and a mono-filamentary CC. The magnetic field distribution of the multi-filamentary CC was obtained by the measurement at $x = 78.31$ m, and that of a mono-filamentary CC was estimated by the equation (1) with the same critical current.

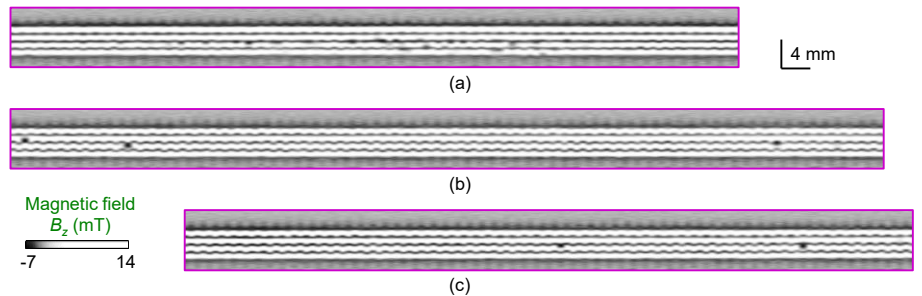


Fig. 7. Remanent magnetic field distributions around the local I_c drops at (a) $x = 22$ m, (b) $x = 80$ m, and (c) $x = 90$ m.

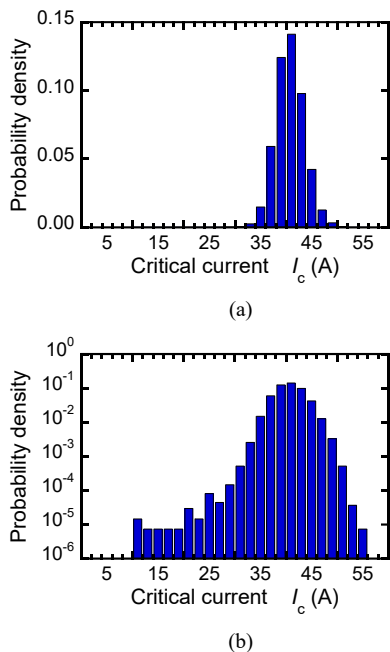


Fig. 8. Histogram with the probability density of local I_c distribution of Filament 3 shown (a) by linear scale and (b) by semi-logarithmic scale.

Fig. 5 shows the results obtained by the RTR-SHPM with the related analyses. Two-dimensional distribution of magnetic field in the remanent state was successfully obtained for such a long multi-filamentary CC; it was confirmed that 4-filamentary structure and the corresponding reduction of magnetization were achieved in this sample. For example, when same critical current as the total critical currents of the four filaments at $x = 78.31$ m was assumed for a mono-filamentary CC, magnetic field distribution could be estimated as shown in Fig. 6; reduction of the magnetization by the multi-filamentary structure could be confirmed.

From the remanent magnetic field distribution, local I_c value at each filament was obtained as a function of longitudinal position. The electric field criterion could be estimated by relaxation measurements [12], and was estimated to be 10^{-8} V/m for this measurement condition: 10,000 times lower electric field criterion than the typical one of 10^{-4} V/m. It can be seen that each filament has non-negligible local I_c drops especially around $x = 22, 80, 90$ m where I_c drops are shown also by the 4-probe-method.

Fig. 7 shows the magnetic field distributions for such locations. The sizes and the locations can be clearly seen in the figure; typical size would be ~ 1 mm. In other words, it is necessary to detect such a small defect from a long CC, and we could do that.

Such I_c drops in each filament resulted in those of total I_c , and could explain the global I_c drops as shown the lower side of Fig. 5. The global I_c was estimated as the current where the averaged electric field became 10^{-4} V/m between voltage tap distance by assuming the electric field at each measurement position by n -value model with a typical value of 30:

$$E = E_c \left(\frac{I}{I_c} \right)^n \quad (2)$$

where E_c is the electric field criterion used for the determination of I_c .

Furthermore, Fig. 8 shows the histogram of local I_c distribution in Filament 3. In the linear plot, minimum I_c looks slightly smaller than the average apparently. However, in fact, it can be seen in the semi-logarithmic plot that there are several positions with even smaller I_c at very small probability density in the order of 10^{-5} . This can be clarified only by a high-resolution measurement for a long CC.

In this way, the RTR-SHPM with the related analyses could detect local I_c drops for each filament as the origin of the global performance reduction of the CC although the TAPESTARTM could not detect them. Furthermore, the locations of the defects could be specified in less than millimeter scale even for a 100-m-long class multi-filamentary CC. This will be crucial information to improve the fabrication process by investigating the origin by site-specified microstructural observation.

IV. CONCLUSION

We applied RTR-SHPM to the diagnostics of a long-length multi-filamentary CC: 113-m-long, 4-mm-wide, and 4-filamentary CC fabricated by Fujikura Ltd. As a result, it was confirmed that the multi-filamentary structure as well as the corresponding magnetization reduction were successfully achieved in such a long-length CC. At the same time, it was also found that there were still some local defects, which affected the global performance of the multi-filamentary CC, although they could not be detected by TAPESTARTM; the locations of the defects could be specified in less than millimeter scale even for a 100-m-long class multi-filamentary CC. These findings will become crucial information for the optimization of fabrication processes of multi-filamentary CCs and for their nondestructive quality assurance.

ACKNOWLEDGMENT

This work was partly supported by “JSPS: KAKENHI (16H02334, 16K14216).

REFERENCES

- [1] Y. Yanagisawa, H. Nakagome, D. Uglietti, T. Kiyoshi, R. Hu, T. Takematsu, T. Takao, M. Takahashi, and H. Maeda, “Effect of YBCO-Coil Shape on the Screening Current-Induced Magnetic Field Intensity,” *IEEE Trans. Appl. Supercond.*, vol. 20, pp. 744-747, 2010.
- [2] M. Zhang, W. Yuan, D. K. Hilton, M. D. Canassy, and U. P. Trociewitz, “Study of second-generation high-temperature superconducting magnets: the self-field screening effect,” *Supercond. Sci. Technol.*, vol. 27, ArtID. 095010, 2014.
- [3] M. C. Ahn, J. Jang, W. S. Lee, S. Hahn, and H. Lee, “Experimental Study on Hysteresis of Screening-Current-Induced Field in an HTS Magnet for NMR Applications,” *IEEE Trans. Appl. Supercond.*, vol. 24, ArtID. 4301605, 2014.
- [4] T. Machi, K. Nakao, T. Kato, T. Hirayama, and K. Tanabe, “Reliable fabrication process for long-length multi-filamentary coated conductors by a laser scribing method for reduction of AC loss,” *Supercond. Sci. Technol.*, vol. 26, ArtID. 105016, 2015.
- [5] I. Kesgin, G. A. Levin, T. J. Haugan, and V. Selvamanickam, “Multifilament, copper-stabilized superconductor tapes with low

- alternating current loss,” *Appl. Phys. Lett.*, vol. 103, ArtID. 252603, 2014.
- [6] A. C. Wulff, M. Solovyov, F. Gömory, A. B. Abrahamsen, O. V. Mishin, A. Usoskin, A. Rutt, J. H. Lundeman, K. Thydén, J. B. Hansen, and J.-C. Grivel, “Two level undercut-profile substrate for filamentary $\text{YBa}_2\text{Cu}_3\text{O}_7$ coated conductors,” *Supercond. Sci. Technol.*, vol. 28, ArtID. 072001, 2015.
- [7] C. Kurihara, S. Fujita, N. Nakamura, M. Igarashi, Y. Iijima, K. Higashikawa, D. Uetsuhara, T. Kiss, M. Iwakuma, “Multi-filamentary REBCO tapes fabricated by scratching a buffer layer along the tape longitudinal direction,” *Physica C*, in press.
- [8] S. Furtner, R. Nemetschek, R. Semerad, G. Sigl, and W. Prusseit, “Reel-to-reel critical current measurement of coated conductors,” *Supercond. Sci. Technol.*, vol. 17, pp. S281-284, 2004.
- [9] K. Higashikawa, K. Shiohara, M. Inoue, T. Kiss, T. Machi, N. Chikumoto, S. Lee, K. Tanabe, T. Izumi, and H. Okamoto, “Noncontact Characterization of In-Plane Distribution of Critical Current Density in Multifilamentary Coated Conductor,” *IEEE Trans. Appl. Supercond.*, vol. 22, ArtID. 9500704, 2012.
- [10] X.-F. Li, M. Kochat, G. Majkic, and V. Selvamanickam, “Critical current density measurement of striated multifilament-coated conductors using a scanning Hall probe microscope,” *Supercond. Sci. Technol.*, vol. 29, ArtID. 085014, 2016.
- [11] K. Higashikawa, K. Katahira, M. Inoue, T. Kiss, Y. Shingai, M. Konishi, K. Ohmatsu, T. Machi, M. Yoshizumi, T. Izumi, and Y. Shiohara, “Nondestructive Diagnostics of Narrow Coated Conductors for Electric Power Applications,” *IEEE Trans. Appl. Supercond.*, vol. 24, ArtID. 6600704, 2014.
- [12] K. Shiohara, K. Higashikawa, M. Inoue, T. Kiss, Y. Iijima, T. Saitoh, M. Yoshizumi, and T. Izumi “Measurement of in-plane magnetic relaxation in RE-123 coated conductors by use of scanning Hall probe microscopy,” *Physica C*, vol. 484, pp. 139-141, 2013.